



Convolutional Neural Network Simplification with Progressive Retraining

Osaku, D.^a, Gomes, J.F.^a, Falcão, A.X.^a

^aState University of Campinas, Brazil

ABSTRACT

Kernel pruning methods have been proposed to speed up, simplify, and improve explanation of convolutional neural network (CNN) models. However, the effectiveness of a simplified model is often below the original one. In this letter, we present new methods based on objective and subjective relevance criteria for kernel elimination in a layer-by-layer fashion. During the process, a CNN model is retrained only when the current layer is entirely simplified, by adjusting the weights from the next layer to the first one and preserving weights of subsequent layers not involved in the process. We call this strategy *progressive retraining*, differently from kernel pruning methods that usually retrain the entire model after each simplification action – e.g., the elimination of one or a few kernels. Our subjective relevance criterion exploits the ability of humans in recognizing visual patterns and improves the designer's understanding of the simplification process. The combination of suitable relevance criteria and progressive retraining shows that our methods can increase effectiveness with considerable model simplification. We also demonstrate that our methods can provide better results than two popular ones and another one from the state-of-the-art using four challenging image datasets.

© 2022 Elsevier Ltd. All rights reserved.

1. Introduction

The simplification of a pretrained neural network involves the elimination of neurons that might cause minor effectiveness loss after retraining (Karnin (1990); LeCun et al. (1990)). These methods have been proposed for decades. When applied to the convolutional neural network (CNN) models, they are often referred to as kernel pruning methods. Such methods can speed up, simplify, and improve the explanation of the models (He et al. (2017); Huang et al. (2018); Augusta and Kathirvalavakumar (2013)), but their effectiveness is often below the original one (Luo et al. (2017); Jordao et al. (2019); Li et al. (2016)).

We have observed that kernel pruning methods usually retrain the entire model after each simplification action – e.g., the elimination of one or a few kernels from a given layer. We call this strategy *complete retraining*. It alters the weights of subsequent layers that have not been involved yet. Given the known problems of retraining deep neural networks, we presume that the accuracy loss in those simplified models is related to complete retraining and the criteria adopted for kernel elimination.

In this letter, we circumvent the problem by presenting kernel pruning methods that operate in a layer-by-layer fashion with effectiveness improvements. The methods include new strategies for (a) kernel elimination and (b) model retraining

after each layer simplification. In (a), we present *objective* and *subjective* kernel relevance criteria. In the objective criterion, lower is the negative impact of a kernel in the cross-entropy loss function higher is its priority for removal. In the subjective criterion, the user (a CNN designer) visualizes a 2D projection (Maaten and Hinton (2008)) of the *mean activation maps* that the kernels generate for each class, and eliminates kernels that cannot separate classes in the projection. Each kernel of a given convolutional layer produces one activation map for each input image. The mean activation map of images from the same class indicates the most relevant regions activated by that kernel. We expect that a relevant kernel activates differently for at least one class. Therefore, a kernel remains in the model when at least one class appears separated from the others in the projection of its mean activation maps (Figure 1). This subjective criterion explores the ability of humans to recognize visual patterns and improves the expert's understanding of the model simplification process. In (b), we present a new strategy, named *progressive retraining*, in which the CNN model is retrained from the layer after the simplified one to layer one by backpropagation. Progressive retraining aims to recover the model's generalization capability before the simplification of the next convolutional layer.

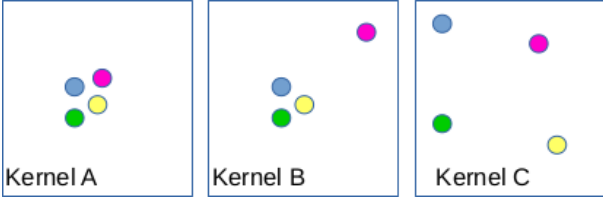


Fig. 1. Hypothetical 2D projections (Maaten and Hinton (2008)) of the mean activation maps of three kernels (A, B, and C) for four color-coded classes. We remove kernel A and keep kernels B and C in the CNN model.

We first discuss related works and emphasize the importance of the above contributions (Section 2). Section 3 describes two new CNN simplification methods that operate in a layer-by-layer fashion based on the proposed kernel relevance criteria and progressive retraining. The experiments first evaluate the advantages of progressive retraining over complete retraining on four challenging image datasets (Section 4). These advantages come with significant efficiency gains over a reference CNN model, Vgg-16 (Simonyan and Zisserman (2014)), and improvements in effectiveness — a rare phenomenon in kernel pruning methods. We finally show the effectiveness gains of the proposed approaches over two popular kernel pruning methods (Li et al. (2016); Hu et al. (2016)) and one approach from the state-of-the-art (Jordao et al. (2019)).

2. Related works

Neural network simplification methods have been investigated for decades. Karnin (1990) estimates the sensitivity of the global error function when removing neurons, and prunes low sensitivity connections. Engelbrecht and Cloete (1996) propose a similar idea by estimating sensitivity at the output of the layer after the one under simplification. Poppi and Massart (1998) adopt a special algorithm to measure the impact of removing a neuron in the training error. Sum et al. (1999) use an extended Kalman filter to measure the importance of a connection weight in a network. Augasta and Kathirvalavakumar (2013) provide a comparative study of neuron pruning methods on real datasets.

The above methods have been focused on multi-layer perceptron (MLP) models. More recently, after the introduction of CNN models, new kernel pruning methods have appeared. They aim at simplifying the CNN architecture by eliminating redundant kernels and/or kernels that can be removed with minor negative impact in accuracy. However, it has been difficult for those methods to obtain significant network simplifications with no accuracy loss (Luo et al. (2017); Jordao et al. (2019); Li et al. (2016)).

According to He et al. (2017), recent advances in CNN acceleration can be divided into three categories: (1) optimized implementations (Vasilache et al. (2014)), (2) weight quantization (Rastegari et al. (2016)), and (3) structured simplification (Jaderberg et al. (2014)). Kernel pruning methods fall into category (3). LeCun et al. (1990), for instance, identify irrelevant connection weights based on their negligible impact in accuracy. Li et al. (2016) determine the importance of each kernel using the L1 norm of the weights and then kernels with

lower values are pruned. By conducting simplification experiments on Vgg-16, ResNet34, ResNet56, and ResNet101, the authors report small losses in accuracy for reduction factors from 20% to 30% of the original number of kernels. Luo et al. (2017) measure the impact of kernel removal at the output of the next layer to identify possible redundant kernels. Kernels that cause smaller changes in the total activation map of the next layer are selected for removal. They report a slight increase in the top-5 accuracy on the ImageNet dataset, when 50% of the kernels in the first 10 layers of Vgg-16 are removed, and a slight decrease in the top-5 accuracy, when fully connected layers are replaced by general average pooling, which represents a considerable simplification of Vgg-16. Other kernel relevance criteria may be based on Taylor expansion (Molchanov et al. (2016)) or the percentage of zero activations (Hu et al. (2016)).

More complex simplification approaches have also been proposed. For instance, Huang et al. (2018) propose pruning agents to detect and eliminate unnecessary kernels. This pruning agent is modeled as a second CNN model which takes the kernel weights of the model under simplification as input and output binary decisions about removing or not kernels. The authors report a loss in accuracy of about 3% after pruning the Vgg-16 and ResNet18 models using the CIFAR-10 dataset. He et al. (2017) employ Lasso regression to determine redundant kernels for pruning and report slight accuracy losses with some simplified CNN models.

More recently, Jordao et al. (2019) estimates the importance of kernels for pruning based on the relationship between classes in a latent space, generated by partial least squares, and their variable importance in projection. They first eliminate kernels in the entire network and then retrain the model. They report considerable simplification without penalizing accuracy.

We present kernel pruning methods that simplify the convolutional layers of a CNN model in a layer-by-layer fashion. Differently from all previous approaches, we retrain the model progressively, without affecting the weights of subsequent layers that have not been involved yet. We also introduce a subjective criterion based on the visual analysis of data projections. By that, we would like to call attention for the importance of using visual analytics in the design of deep neural networks. The strategy seems promising to guide human actions in the machine learning loop, such that the resulting models are as simple and effective as possible for a given problem. In this context, there is a lack of interactive methods for the construction of deep neural networks.

Visual analytics have been successfully employed to understand neural networks and explain their decisions (Morch et al. (1995); Duch (2004); Zeiler and Fergus (2014); Rauber et al. (2017); Hohman et al. (2020)). It has also been used in the design of deep neural network models (Pezzotti et al. (2018); Garcia et al. (2019)). Pezzotti et al. (2018) present a system, named DeepEyes, to support the design of such models, and Garcia et al. (2019) show a first method to build a simplified CNN model in a layer-by-layer fashion. They introduce a kernel selectivity criterion based on the visual analysis of the *activation occurrence maps* for each class. That is, by counting the positive activations for input images from each class, the user can

visualize those activation maps as 2D images and choose the kernels with different activation patterns among classes. The method is limited by the number of classes and the 2D dimension of the activation maps (2D input images). In the proposed subjective criterion, we use 2D projections to allow more classes and overcome the limitation about the dimension of the activation maps. However, we are still limited to reasonable numbers of classes, layers, and kernels per layer.

3. Pruning with progressive retraining

This section presents two approaches to simplify CNNs based on kernel relevance criteria followed by progressive retraining (fine-tuning) in a layer by layer fashion (Figure 2). One may conceptually divide a CNN for image classification into three parts: (1) a sequence of convolutional layers, with each layer containing convolution, activation, and optional operations (e.g., pooling, batch normalization) useful for feature extraction; (2) fully connected layers for feature space reduction, which discover the neurons specialized in each class (Rauber et al. (2017)); and (3) a decision layer for final classification, being (2) and (3) known as a MLP classifier. We have applied the following procedures to simplify pre-trained CNNs based on the analysis of each convolutional layer’s output.

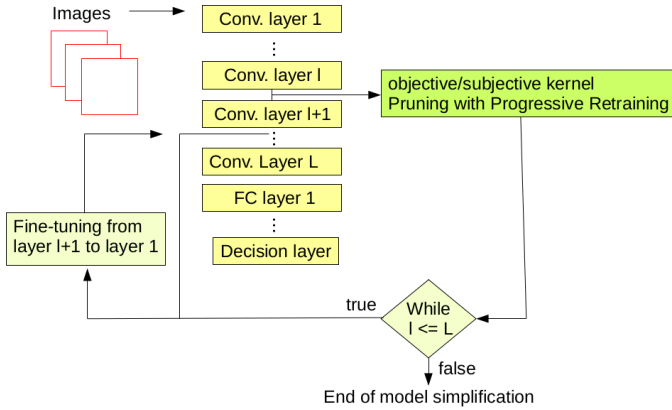


Fig. 2. Kernel pruning with progressive retraining using an objective/subjective criterion. Progressive retraining for a simplified layer l starts from the output of layer $l + 1$ to layer 1 by backpropagation.

3.1. Objective pruning

The first approach, named *objective Pruning with Progressive Retraining* (oPPR), eliminates kernels of a given convolutional layer l based on an *objective relevance criterion* and fine-tunes the network by backpropagation during x epochs (e.g., $x = 40$) from layer $l + 1$ to layer 1, aiming to recover its previous activations at the output of layer $l + 1$. This process starts at layer 1 and proceeds until the simplification of the last convolutional layer L , when the fine-tuning involves the weight optimization from the first fully connected layer $L + 1$ to layer 1.

In this approach, the relevance of a kernel k is related to its impact on the neural network’s loss function. We use cross-entropy as loss function — higher is the loss, when removing a

kernel k from a layer l , more critical the kernel k is for layer l . Given that, for a layer l , one can remove either a given number of the most irrelevant kernels or the kernels whose relevance is below a given threshold.

Once a set $\mathcal{M}_l \subset \mathcal{K}_l$ of kernels have been removed from the original kernel set \mathcal{K}_l of layer l , we apply backpropagation to refine the weights from layer $l + 1$ to layer 1. The loss function in this case is the mean square difference of the activation values obtained with and without \mathcal{M}_l at the output of layer $l + 1$. That is, let I be an input image to the network, \mathcal{X} be the set of training images, $A_{l+1}(I, \mathcal{K}_l) \in \mathbb{R}^{n_{l+1}}$ be the output of layer $l + 1$, after ReLu and, whenever the case, after pooling, with n_{l+1} activation values, as a result from the input I , and $A_{l+1}(I, \mathcal{K}_l \setminus \mathcal{M}_l) \in \mathbb{R}^{n_{l+1}}$ be the same without \mathcal{M}_l . The loss function for progressive retraining is defined as

$$\bar{D}_{l+1} = \frac{1}{|\mathcal{X}|} \sum_{I \in \mathcal{X}} \|A_{l+1}(I, \mathcal{K}_l) - A_{l+1}(I, \mathcal{K}_l \setminus \mathcal{M}_l)\|_2. \quad (1)$$

3.2. Subjective pruning

The second approach, named *subjective Pruning with Progressive Retraining* (sPPR), works similarly to oPPR, except for the kernel relevance criterion. In this case, an expert in the design of neural networks visualizes 2D non-linear projections of *mean activation maps* and decides which kernels are the most relevant, according to the expert’s subjective judgment of the separation in the projection among the mean activation maps of the classes for each given kernel. One should expect that a relevant kernel can separate at least one class from the others (Figure 3).

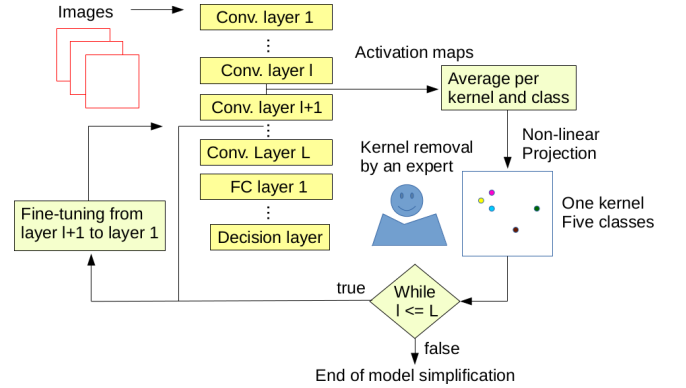


Fig. 3. sPPR: for each convolutional layer l , the expert analyzes the projections of the mean activation maps of the classes from each kernel, and eliminates kernels that form one cluster of points in the projection.

Let $\mathcal{X}_j \subset \mathcal{X}$ be the set of training images from the class $j \in \{1, 2, \dots, c\}$. Let $A_{l,k,j}(I) \in \mathbb{R}^n$ be a map with $n < n_l$ activations at the output of layer l as a consequence of using an input image I from class j and a kernel k up to layer l . Note that these are the activations from the subset of the n_l activations, which result from the convolution with kernel k only. One mean activation map $\bar{A}_{l,k,j}$ from kernel k and for each class j can be obtained from the output of layer l as

$$\bar{A}_{l,k,j} = \frac{1}{|\mathcal{X}_j|} \sum_{I \in \mathcal{X}_j} A_{l,k,j}(I). \quad (2)$$

We use the t-SNE algorithm (Maaten and Hinton (2008)) to project the mean activation maps $\bar{A}_{l,k,j}$ for all kernels k and classes j at the output of layer l in the 2D space (Figure 4a). Nevertheless, the expert analyzes the class projections of each kernel separately. For a reasonable number of kernels (e.g., 512), the user can quickly visualize only c points in 2D per time from each kernel k as an indication of how it discriminates among the images of the c classes (Figures 4b-4d). If the points are very close to each other, forming one cluster in 2D, we may conclude that the kernel cannot discriminate between the classes. A kernel k remains in layer l when it can separate at least one class from the others. The separation between classes in the 2D projection is a subjective criterion that depends on the expert’s visual analysis only.

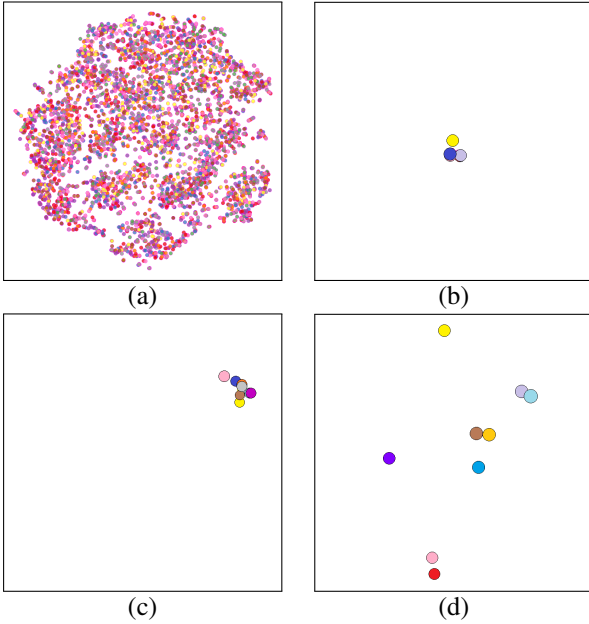


Fig. 4. For a layer with 512 kernels and a dataset with $c = 9$ classes. The t-SNE projection of the mean activation maps (a) from all kernels and (b-d) from three distinct kernels. The color indicates the class of images used to create the mean activation maps. The kernels in (b) and (c) are candidates for removal, while the kernel in (d) is a relevant one.

After eliminating those irrelevant kernels from layer l , we apply backpropagation to refine the weights from layer $l + 1$ to 1, as described for the *oPPR* approach. It is also possible to remove redundant kernels among the relevant ones. Redundant kernels have similar weights, so the projection of their weight vectors forms one cluster of points in 2D. Although this may further simplify the CNN, we have evaluated only the elimination of irrelevant kernels.

3.3. After network simplification

After simplification, the entire simplified network is retrained with y epochs (e.g., $y = 50$). This process starts with random weights in the fully connected layers (MLP classifier) (Glorot and Bengio (2010)) but only fine-tunes the weights of the convolutional layers, which resulted from progressive retraining. We have observed that the progressive retraining can recover

Table 1. Number of classes, pixels and bands (resolution), training samples, and testing samples in each dataset.

| Dataset | Number of Classes | Image Resolution | Training samples | Testing samples | Total of samples |
|---------|-------------------|------------------|------------------|-----------------|------------------|
| EGG-9 | 9 | 200x200x3 | 1265 | 10156 | 11421 |
| LAR-2 | 2 | 200x200x3 | 478 | 960 | 1438 |
| PRO-7 | 7 | 200x200x3 | 3733 | 29902 | 33635 |
| STL-10 | 10 | 96x96x3 | 3900 | 7800 | 11700 |

the generalization capability of the CNN better than retraining the entire network after each layer simplification, as recommended in most works in (Li et al. (2016); Hu et al. (2016); He et al. (2017); Jordao et al. (2019)).

4. Experiments, results, and discussion

To evaluate the simplification of CNNs using the *oPPR* and *sPPR* approaches, we divided the experiments into two parts. We use the Vgg-16 (Simonyan and Zisserman (2014)) model as reference, pre-trained on the ImageNet dataset (Deng et al. (2009)) and adjusted to the training set of each dataset below:

- EGG-9: it is a private dataset with images of the eight most common species of helminth eggs in Brazil and one diverse class of fecal impurities.
- PRO-7: it is a private dataset with images of the six most common species of protozoa cysts in Brazil and one diverse class of fecal impurities.
- LAR-2: it is a private dataset with images of *S. stecoralis* (helminth larvae) and fecal impurities.
- STL-10: it is a well known public dataset with natural images, with considerable variations among objects that define a same class (Coates et al. (2011)).

In each dataset of intestinal parasites, EGG-9, PRO-7, and LAR-2, fecal impurities contain examples that are very similar in texture and shape to those of other classes, which makes these datasets very challenging. These datasets belong to a project for the automation of the diagnosis of intestinal parasites (Suzuki et al. (2013); Suzuki et al. (2013b); Saito et al. (2015); Peixinho et al. (2015)).

For more statistically reliable results, we divided each dataset into five random splits of training and testing images, respectively, as described in Table 1. To fine-tune Vgg-16 in each dataset, we used 50 epochs, learning rate $1e^{-5}$, and reinitialized the weights of its fully connected layers using the method in (Glorot and Bengio (2010)).

We divide the experiments into two parts and discuss the pros and cons of *oPPR* and *sPPR* afterwards.

4.1. The impact of progressive retraining

First, we evaluate the impact of the progressive retraining after each layer simplification by using variants of *oPPR* and *sPPR*, which adopt retraining of the entire network with a single epoch, as in other works (Li et al. (2016); Hu et al. (2016); He et al. (2017); Jordao et al. (2019)). For that, the variants

Table 2. The proposed approaches, oPPR and sPPR, are first compared with their variants, oPCR and sPCR, that adopt retraining of the entire network after each layer simplification, as recommended in He et al. (2017); Jordao et al. (2019).

| Criterion | Retraining | |
|------------|------------|-------------|
| | Complete | Progressive |
| Objective | oPCR | oPPR |
| Subjective | sPCR | sPPR |

Table 3. Learning rates for progressive retraining.

| Layer | Name | N. of Kernels | Learn. rate |
|-------|---------------|---------------|-------------|
| 1 | block1_conv_1 | 64 | $1e^{-5}$ |
| 2 | block1_conv_2 | 64 | $1e^{-6}$ |
| 3 | block2_conv1 | 128 | $1e^{-6}$ |
| 4 | block2_conv2 | 128 | $1e^{-7}$ |
| 5 | block3_conv1 | 256 | $1e^{-7}$ |
| 6 | block3_conv2 | 256 | $1e^{-7}$ |
| 7 | block3_conv3 | 256 | $1e^{-8}$ |
| 8 | block4_conv1 | 512 | $1e^{-8}$ |
| 9 | block4_conv2 | 512 | $1e^{-8}$ |
| 10 | block4_conv3 | 512 | $1e^{-8}$ |
| 11 | block5_conv1 | 512 | $1e^{-8}$ |
| 12 | block5_conv2 | 512 | $1e^{-8}$ |
| 13 | block5_conv3 | 512 | $1e^{-8}$ |

of oPPR and sPPR with complete retraining (fine-tuning) after each layer simplification are named oPCR (*Objective Pruning with Complete Retraining*) and sPCR (*Subjective Pruning with Complete Retraining*), respectively. Table 2 presents the four approaches compared in this first experimental section.

In oPPR and sPPR, we use 40 epochs for progressive retraining and fixed learning rates along the epochs. To fine-tune from layer $l + 1$ to layer 1, the learning rate is fixed as described in Table 3, depending on the number of kernels of Vgg-16 at each convolutional layer l . Lower learning rates are used as higher is the number of kernels.

After network simplification, the fully convolutional layers (the MLP classifier) are reinitialized with random weights (Glorot and Bengio (2010)) for retraining and the weights of the simplified convolutional layers are refined. This retraining process uses 50 epochs and learning rate $1e^{-5}$ in all approaches: oPPR, sPPR, oPCR, and sPCR.

Tables 4-7 present the results of comparison among the four approaches on the datasets EGG-9, PRO-7, LAR-2, and STL-10, respectively. One may observe that, except for two cases (oPPR in EGG-9 and sPPR in LAR-2), oPPR and sPPR could simplify Vgg-16 with some effectiveness gain (in accuracy and Cohen kappa) and considerable efficiency gain, as measured by the percentage of reduction in the number of kernels and GFLOPS. For the objective approaches, progressive retraining (oPPR) is consistently better than complete retraining (oPCR). In the subjective approaches, the expert is usually more restrained and eliminates considerably fewer kernels than the objective approaches. Nevertheless, the reduction in the number of kernels and GFLOPS with effectiveness gain is still significant in sPCR and sPPR.

Table 4. Impact of the progressive retraining (oPPR and sPPR) after each layer simplification over complete retraining (oPCR and sPCR) and the original network (Vgg-16) on the EGG-9 dataset.

| | Accuracy | Cohen Kappa | GFLOPs reduction (%) | Kernel reduction (%) |
|--------|------------------|------------------|----------------------|----------------------|
| Vgg-16 | 97.65 ± 0.31 | 94.00 ± 0.79 | 0.00 | 0.00 |
| oPCR | 96.90 ± 0.24 | 92.02 ± 1.09 | 74.42 | 50.00 |
| oPPR | 97.62 ± 0.10 | 93.94 ± 0.26 | 74.42 | 50.00 |
| sPCR | 97.83 ± 0.01 | 94.43 ± 0.05 | 27.33 | 9.42 |
| sPPR | 97.79 ± 0.20 | 94.34 ± 0.53 | 54.53 | 21.44 |

Table 5. Impact of the progressive retraining (oPPR and sPPR) after each layer simplification over complete retraining (oPCR and sPCR) and the original network (Vgg-16) on the PRO-7 dataset.

| | Accuracy | Cohen Kappa | GFLOPs reduction (%) | Kernel reduction (%) |
|--------|------------------|------------------|----------------------|----------------------|
| Vgg-16 | 96.74 ± 0.15 | 91.93 ± 0.36 | 0.00 | 0.00 |
| oPCR | 95.93 ± 0.48 | 89.91 ± 1.15 | 74.42 | 50.00 |
| oPPR | 97.11 ± 0.18 | 92.83 ± 0.41 | 74.42 | 50.00 |
| sPCR | 97.01 ± 0.37 | 92.61 ± 0.88 | 29.37 | 10.52 |
| sPPR | 97.05 ± 0.21 | 92.68 ± 0.54 | 36.64 | 12.06 |

Table 6. Impact of the progressive retraining (oPPR and sPPR) after each layer simplification over complete retraining (oPCR and sPCR) and the original network (Vgg-16) on the LAR-2 dataset.

| | Accuracy | Cohen Kappa | GFLOPs reduction (%) | Kernel reduction (%) |
|--------|------------------|------------------|----------------------|----------------------|
| Vgg-16 | 97.33 ± 0.81 | 89.65 ± 3.29 | 0.00 | 0.00 |
| oPCR | 96.24 ± 0.89 | 85.83 ± 2.70 | 74.42 | 50.00 |
| oPPR | 97.49 ± 0.50 | 90.38 ± 2.03 | 74.42 | 50.00 |
| sPCR | 97.39 ± 0.27 | 90.01 ± 1.08 | 38.07 | 16.41 |
| sPPR | 97.22 ± 0.66 | 89.32 ± 2.87 | 63.93 | 27.82 |

Table 7. Impact of the progressive retraining (oPPR and sPPR) after each layer simplification over complete retraining (oPCR and sPCR) and the original network (Vgg-16) on the STL-10 dataset.

| | Accuracy | Cohen Kappa | GFLOPs reduction (%) | Kernel reduction (%) |
|--------|------------------|------------------|----------------------|----------------------|
| Vgg-16 | 77.89 ± 2.13 | 75.43 ± 2.37 | 0.00 | 0.00 |
| oPCR | 73.68 ± 0.98 | 70.75 ± 1.09 | 74.25 | 50.00 |
| oPPR | 79.24 ± 1.74 | 76.93 ± 1.94 | 74.25 | 50.00 |
| sPCR | 80.95 ± 2.15 | 78.83 ± 2.39 | 0.20 | 3.85 |
| sPPR | 79.81 ± 1.33 | 77.57 ± 1.48 | 12.61 | 5.97 |

Table 8. Mean accuracy with the elimination of 50% of the kernels in the convolutional layers of Vgg-16. The best results are shown in bold.

| | EGG-9 | PRO-7 | LAR-2 | STL-10 |
|----------------------|------------------------------------|------------------------------------|------------------------------------|------------------------------------|
| Vgg-16 | 97.65 \pm 0.31 | 96.74 \pm 0.15 | 97.33 \pm 0.81 | 77.89 \pm 2.13 |
| Li et al. (2016) | 94.48 \pm 0.66 | 93.29 \pm 0.46 | 95.98 \pm 0.66 | 74.54 \pm 2.19 |
| Hu et al. (2016) | 96.90 \pm 0.21 | 96.03 \pm 0.34 | 95.6 \pm 0.81 | 73.55 \pm 1.08 |
| Jordao et al. (2019) | 96.71 \pm 0.47 | 94.83 \pm 0.46 | 96.85 \pm 0.30 | 75.89 \pm 1.18 |
| oPPR | 97.62 \pm 0.10 | 97.11 \pm 0.18 | 97.49 \pm 0.50 | 79.24 \pm 1.74 |
| sPPR | 97.79 \pm 0.20 | 97.05 \pm 0.21 | 97.22 \pm 0.66 | 79.81 \pm 1.33 |

Table 9. Mean Cohen kappa with the elimination of 50% of the kernels in the convolutional layers of Vgg-16.

| | EGG-9 | PRO-7 | LAR-2 | STL-10 |
|----------------------|------------------------------------|------------------------------------|------------------------------------|------------------------------------|
| Vgg-16 | 94.00 \pm 0.78 | 91.93 \pm 0.36 | 89.65 \pm 3.29 | 75.43 \pm 2.37 |
| Li et al. (2016) | 85.51 \pm 1.89 | 83.39 \pm 0.83 | 84.30 \pm 2.47 | 71.72 \pm 2.44 |
| Hu et al. (2016) | 92.01 \pm 0.61 | 90.19 \pm 0.80 | 83.26 \pm 3.46 | 70.61 \pm 1.20 |
| Jordao et al. (2019) | 91.61 \pm 1.24 | 87.40 \pm 0.98 | 87.84 \pm 1.35 | 73.21 \pm 1.32 |
| oPPR | 93.94 \pm 0.26 | 92.83 \pm 0.41 | 90.38 \pm 2.03 | 76.93 \pm 1.94 |
| sPPR | 94.34 \pm 0.53 | 92.68 \pm 0.54 | 89.32 \pm 2.87 | 77.57 \pm 1.48 |

4.2. Comparison with other methods

In this section, we compare the proposed approaches (oPPR and sPPR) with other network simplification techniques. These techniques usually differ in two important aspects: (a) the relevance criterion to eliminate kernels and (b) the retraining strategy of the network after each layer simplification. We selected the methods in Li et al. (2016), Hu et al. (2016), and Jordao et al. (2019) for our comparative analysis. In Li et al. (2016), the relevance of a kernel is measured by the sum of the absolute values of its weights. In Hu et al. (2016), the kernels that generate more outputs with no activation are considered less relevant. In Jordao et al. (2019), the kernels are selected using partial least squares and variable importance in projection. For a fair comparison, the kernels were pruned using iterative pruning with 5 iterations of 10% of pruning ratio, which reduces in 34.39% the number of kernels in the convolutional layers. All baselines adopted their original protocols for kernel pruning followed by complete retraining. The first two network simplification approaches are popular baselines for several works.

In our case, we have fixed at 50% the percentage of reduction in the number of kernels per layer for the objective approach, and repeated the results of the previous experiment for sPPR and the original Vgg-16, as references. For each layer, we eliminate 50% of irrelevant kernels and apply progressive retraining.

At the end of the simplification process, all simplified models are retrained with 50 epochs, fixed learning rate $1e^{-5}$, and reinitialized fully connected layers (Glorot and Bengio (2010)).

Tables 8 and 9 show the results of this experiment on each dataset using accuracy and Cohen kappa as effectiveness measures, respectively. The results indicate that oPPR (and sPPR with less efficiency gain than oPPR) can be considerably more effective than the baselines, especially in Cohen kappa. This result is particularly important, because these datasets are unbalanced and Cohen kappa can penalize errors in small classes.

4.3. Discussion

The experiments have demonstrated that the proposed progressive retraining can provide higher effectiveness gains than

the complete retraining usually adopted in network simplification (Li et al. (2016); Hu et al. (2016); He et al. (2017); Jordao et al. (2019)). When simplifying networks, it is typical for the simplified version to be less effective than the original one, as observed for the methods in (Li et al. (2016); Hu et al. (2016); Jordao et al. (2019)) in all datasets. On the other hand, oPPR and sPPR, consistently presented effectiveness gains over Vgg-16 (being oPPR in EGG-9 and sPPR in LAR-2, the exceptions for 50% of kernel elimination). Given the considerable reduction in the number of kernels and GFLOPS, we may conclude that oPPR and sPPR are relevant contributions to the literature of network simplification.

Although oPPR, with a more aggressive kernel elimination, sometimes presented better performance than sPPR, the expert involvement in deep learning has several advantages. First, the expert can better understand the role of each element of the model and, perhaps, better explain its decisions (Raubert et al. (2017)). Second, the expert can intervene in the project of the network, as demonstrated by sPPR. Visual analytics techniques, such as t-SNE, play a central role in facilitating communication between machines and humans. They are known as essential tools to improve understanding of the machine learning process. However, we believe they can go beyond and let the user intervene to improve the machine learning process (Raubert et al. (2018); Benato et al. (2018)). In this sense, sPPR can improve with additional information about objective relevance measures to guide the expert’s actions when eliminating kernels. A drawback in sPPR, however, is the limitation to reasonable numbers of classes, layers, and kernels per layer. On the other hand, oPPR completely relies on the objective relevance measure and eliminates a given and fixed percentage of kernels per layer. It seems that, with the expert in the process, some better criterion could be devised to eliminate an adaptive number of irrelevant kernels per layer.

5. Conclusion

We have presented two solutions for CNN simplification, named oPPR and sPPR, which explore objective and subjective kernel relevance criteria, respectively, and perform progressive retraining to adjust the model’s weights by preserving the weights of subsequent layers not involved in the simplification process. Progressive retraining has shown improvements over complete retraining, usually adopted in kernel pruning methods. The proposed methods have achieved considerable network simplification with effectiveness gains over the original model. They can also be more effective than two popular methods and one approach from the state-of-the-art. We may then conclude that oPPR and sPPR are relevant contributions to the literature of kernel pruning methods.

We are now interested in investigating methods to construct CNNs in a layer-by-layer fashion by exploring objective and subjective kernel relevance criteria. In the context of the diagnosis of intestinal parasites, we intend to create more effective models with considerably simplified architectures.

6. Acknowledgments

The authors thank financial support from FAPESP (Proc. 2017/12974-0 and 2014/12236-1) and CNPq (Proc. 303808/2018-7).

References

- Augasta, M.G., Kathirvalavakumar, T., 2013. Pruning algorithms of neural networks—a comparative study. *Central European Journal of Computer Science* 3, 105–115.
- Benato, B.C., Telea, A.C., Falcão, A.X., 2018. Semi-supervised learning with interactive label propagation guided by feature space projections, in: 2018 31st SIBGRAPI Conference on Graphics, Patterns and Images (SIBGRAPI), pp. 392–399. doi:<https://doi.org/10.1109/SIBGRAPI.2018.00057>.
- Coates, A., Ng, A., Lee, H., 2011. An analysis of single-layer networks in unsupervised feature learning, in: *Proceedings of the fourteenth international conference on artificial intelligence and statistics*, pp. 215–223.
- Deng, J., Dong, W., Socher, R., Li, L.J., Li, K., Fei-Fei, L., 2009. ImageNet: A Large-Scale Hierarchical Image Database, in: *CVPR09*.
- Duch, W., 2004. Visualization of hidden node activity in neural networks: I. visualization methods, in: Rutkowski, L., Siekmann, J.H., Tadeusiewicz, R., Zadeh, L.A. (Eds.), *Artificial Intelligence and Soft Computing - ICAISC 2004*, Springer Berlin Heidelberg, Berlin, Heidelberg. pp. 38–43.
- Engelbrecht, A.P., Cloete, I., 1996. A sensitivity analysis algorithm for pruning feedforward neural networks, in: *Proceedings of International Conference on Neural Networks (ICNN'96)*, pp. 1274–1278 vol.2.
- Garcia, R., Falcão, A.X., Telea, A.C., da Silva, B.C., Tørresen, J., Dihl Comba, J.L., 2019. A methodology for neural network architectural tuning using activation occurrence maps, in: 2019 International Joint Conference on Neural Networks (IJCNN), pp. 1–10. doi:10.1109/IJCNN.2019.8852223.
- Glorot, X., Bengio, Y., 2010. Understanding the difficulty of training deep feedforward neural networks, in: *Proceedings of the thirteenth international conference on artificial intelligence and statistics*, pp. 249–256.
- He, Y., Zhang, X., Sun, J., 2017. Channel pruning for accelerating very deep neural networks, in: *Proceedings of the IEEE International Conference on Computer Vision*, pp. 1389–1397.
- Hohman, F., Park, H., Robinson, C., Chau, D.H.P., 2020. Summit: Scaling deep learning interpretability by visualizing activation and attribution summarizations. *IEEE Transactions on Visualization and Computer Graphics*, 1096–1106.
- Hu, H., Peng, R., Tai, Y.W., Tang, C.K., 2016. Network trimming: A data-driven neuron pruning approach towards efficient deep architectures. *arXiv preprint arXiv:1607.03250*.
- Huang, Q., Zhou, K., You, S., Neumann, U., 2018. Learning to prune filters in convolutional neural networks, in: 2018 IEEE Winter Conference on Applications of Computer Vision, pp. 709–718.
- Jaderberg, M., Vedaldi, A., Zisserman, A., 2014. Speeding up convolutional neural networks with low rank expansions. *arXiv preprint arXiv:1405.3866*.
- Jordao, A., Kloss, R., Yamada, F., Schwartz, W.R., 2019. Pruning deep neural networks using partial least squares, in: *British Machine Vision Conference (BMVC) Workshops: Embedded AI for Real-Time Machine Vision*.
- Karnin, E.D., 1990. A simple procedure for pruning back-propagation trained neural networks. *IEEE Transactions on Neural Networks* 1, 239–242.
- LeCun, Y., Denker, J.S., Solla, S.A., 1990. Optimal brain damage, in: *Advances in neural information processing systems*, pp. 598–605.
- Li, H., Kadav, A., Durdanovic, I., Samet, H., Graf, H.P., 2016. Pruning filters for efficient convnets. *arXiv preprint arXiv:1608.08710*.
- Luo, J.H., Wu, J., Lin, W., 2017. Thinet: A filter level pruning method for deep neural network compression, in: *Proceedings of the IEEE international conference on computer vision*, pp. 5058–5066.
- Maaten, L.v.d., Hinton, G., 2008. Visualizing data using t-sne. *Journal of machine learning research* 9, 2579–2605.
- Molchanov, P., Tyree, S., Karras, T., Aila, T., Kautz, J., 2016. Pruning convolutional neural networks for resource efficient inference. *arXiv preprint arXiv:1611.06440*.
- Morch, N.J.S., Kjems, U., Hansen, L.K., Svarer, C., Law, I., Lautrup, B., Strother, S., Rehm, K., 1995. Visualization of neural networks using saliency maps, in: *Proceedings of ICNN'95 - International Conference on Neural Networks*, pp. 2085–2090 vol.4.
- Peixinho, A.Z., Martins, S., Vargas, J.E., Falcão, A.X., Gomes, J.F., Suzuki, C.T.N., 2015. Diagnosis of human intestinal parasites by deep learning, in: *Proc. of Computational Vision and Medical Image Processing V (VipImage)*, pp. 107–112.
- Pezzotti, N., Höllt, T., Van Gemert, J., Lelieveldt, B.P.F., Eisemann, E., Vılanova, A., 2018. Deepeyes: Progressive visual analytics for designing deep neural networks. *IEEE Transactions on Visualization and Computer Graphics* 24, 98–108.
- Poppi, R., Massart, D., 1998. The optimal brain surgeon for pruning neural network architecture applied to multivariate calibration. *Analytica Chimica Acta* 375, 187 – 195. URL: <http://www.sciencedirect.com/science/article/pii/S0003267098004620>, doi:[https://doi.org/10.1016/S0003-2670\(98\)00462-0](https://doi.org/10.1016/S0003-2670(98)00462-0).
- Rastegari, M., Ordonez, V., Redmon, J., Farhadi, A., 2016. Xnor-net: ImageNet classification using binary convolutional neural networks, in: Leibe, B., Matas, J., Sebe, N., Welling, M. (Eds.), *Computer Vision – ECCV 2016*, Springer International Publishing, Cham. pp. 525–542.
- Rauber, P., Falcão, A., Telea, A., 2018. Projections as visual aids for classification system design. *Information Visualization* 17, 282–305. doi:10.1177/1473871617713337.
- Rauber, P.E., Fadel, S.G., Falcão, A.X., Telea, A.C., 2017. Visualizing the hidden activity of artificial neural networks. *IEEE Transactions on Visualization and Computer Graphics* 23, 101–110.
- Saito, P., Suzuki, C., Gomes, J., de Rezende, P., Falcão, A., 2015. Robust active learning for the diagnosis of parasites. *Pattern Recognition* 48, 3572 – 3583. doi:<https://doi.org/10.1016/j.patcog.2015.05.020>.
- Simonyan, K., Zisserman, A., 2014. Very deep convolutional networks for large-scale image recognition. *CoRR abs/1409.1556*.
- Sum, J., Chi-Sing Leung, Young, G.H., Wing-Kay Kan, 1999. On the kalman filtering method in neural network training and pruning. *IEEE Transactions on Neural Networks* 10, 161–166. doi:10.1109/72.737502.
- Suzuki, C.T.N., Gomes, J.F., Falcão, A.X., Papa, J.P., Hoshino-Shimizu, S., 2013. Automatic segmentation and classification of human intestinal parasites from microscopy images. *IEEE Transactions on Biomedical Engineering* 60, 803–812.
- Suzuki, C.T.N., Gomes, J.F., Falcão, A.X., Shimizu, S.H., Papa, J.P., 2013b. Automated diagnosis of human intestinal parasites using optical microscopy images, in: *IEEE International Symposium on Biomedical Imaging*, pp. 460–463.
- Vasilache, N., Johnson, J., Mathieu, M., Chintala, S., Piantino, S., LeCun, Y., 2014. Fast convolutional nets with fbfft: A gpu performance evaluation. *arXiv preprint arXiv:1412.7580*.
- Zeiler, M.D., Fergus, R., 2014. Visualizing and understanding convolutional networks, in: Fleet, D., Pajdla, T., Schiele, B., Tuytelaars, T. (Eds.), *Computer Vision – ECCV 2014*, Springer International Publishing, Cham. pp. 818–833.